

X-Ray/Gamma-Ray Observations of the PSR B1259–63/SS 2883 system near Apastron

M. Hirayama¹

*Santa Cruz Institute for Particle Physics, University of California, Santa Cruz, Santa Cruz, CA 95064;
hirayama@scipp.ucsc.edu*

L. R. Cominsky

Department of Physics and Astronomy, Sonoma State University, Rohnert Park, CA 94928; lynncc@charmian.sonoma.edu

V. M. Kaspi

*Center for Space Research and Department of Physics, Massachusetts Institute of Technology,
Cambridge, MA 02139; vicky@space.mit.edu*

F. Nagase

*The Institute of Space and Astronautical Science, 1-1 Yoshinodai 3-chome, Sagamihara, Kanagawa 229,
Japan; nagase@astro.isas.ac.jp*

M. Tavani

*Columbia Astrophysics Laboratory, New York, NY 10027
IFCTR-CNR, via Bassini 15, I-20133 Milano, Italy; tavani@astro.columbia.edu*

N. Kawai

*The Institute of Physical and Chemical Research, 2-1 Hirosawa, Wako, Saitama 351-01, Japan;
kawai@postman.riken.go.jp*

and

J. E. Grove

E. O. Hulburt Center for Space Research, U. S. Naval Research Laboratory, MS 7650, Washington, D.C. 20375; grove@osseq.nrl.navy.mil

¹Research Fellow, the Japan Society for the Promotion of Science for Young Scientists

ABSTRACT

We report the results from X-ray and hard X-ray observations of the PSR B1259–63/SS 2883 system with the *ASCA* and *CGRO* satellites, performed between 1995 February and 1996 January when the pulsar was near apastron. The system was clearly detected in each of the two *ASCA* observations with luminosity in the 1–10 keV band of $L_X = (9 \pm 3) \times 10^{32} (d/2 \text{ kpc})^2 \text{ erg s}^{-1}$, while CGRO/OSSE did not detect significant hard X-rays from the system. X-ray spectra obtained with *ASCA* are well-fit by a single power-law spectrum with a photon index of 1.6 ± 0.3 . No pulsations were detected in either the *ASCA* or the OSSE data. We combine all existing X-ray and hard X-ray observations and present the orbital modulation in the luminosity and photon index for the entire orbit. The results are in agreement with predictions based on a synchrotron emission model from relativistic particles in a shocked pulsar wind interacting with the gaseous outflow from the Be star.

Subject headings: binaries: eclipsing — pulsars: individual (PSR B1259–63) — stars: emission line, Be — stars: individual (SS 2883) — stars: neutron — X-rays: stars

1. Introduction

The PSR B1259–63/SS 2883 system is a binary consisting of the radio pulsar PSR B1259–63 and the Be star SS 2883. PSR B1259–63 is a 48 ms radio pulsar, discovered by Johnston et al. (1992a). The pulsar’s parameters were determined by Manchester et al. (1995) using radio timing observations with the Parkes 64-m radio telescope, covering the two periastron passages in 1990 and in 1994. The radio timing observations have shown that the pulsar is in a 3.4 yr, binary orbit with eccentricity $e = 0.86$. Further radio observations with the Parkes telescope suggest that the binary orbit may be precessing by the quadrupole moment of the tilted companion star (Wex et al. 1998). The companion star has been identified as the 10th magnitude B2e star SS 2883 from optical observations, and the mass and radius of SS 2883 were estimated to be $\sim 10 M_{\odot}$ and $\sim 6 R_{\odot}$, respectively (Johnston et al. 1992b).

From the dispersion measure (DM) of the pulsar and a model for the galactic electron distribution (Taylor & Cordes 1993), the estimated distance to the source is 4.6 kpc, although DM-derived distances are uncertain often to a factor of ~ 2 . Johnston et al. (1994) argue on the basis of optical photometric observations that the distance to SS 2883 cannot be greater than 1.5 kpc. In this paper we adopt a compromise distance of 2 kpc.

The first attempt to detect X-rays from the PSR B1259–63/SS 2883 system was in observations made using the *Ginga* satellite in 1991. However, *Ginga* failed to detect significant X-ray emission from the system (Makino & Aoki 1994). The first low-level X-ray detection was by Cominsky, Roberts, & Johnston (1994) who observed the system just after apastron using *ROSAT* in September 1992 (“*ROSAT* obs 2” and “*ROSAT* obs 3” in Fig. 1). The X-ray luminosity in the 1 – 10 keV band during these observations can be derived from the *ROSAT* results as (0.07 – 2)

$\times 10^{33}(d/2 \text{ kpc})^2 \text{ erg s}^{-1}$ for *ROSAT* obs 2 and $(0.3 - 1.5) \times 10^{33}(d/2 \text{ kpc})^2 \text{ erg s}^{-1}$ for *ROSAT* obs 3, respectively, assuming the spectral parameters given by Cominsky, Roberts, & Johnston (1994). A subsequent analysis by Greiner, Tavani, & Belloni (1995) of archival *ROSAT* data taken just before apastron in February 1992 (“*ROSAT* obs 1” in Fig. 1), reveals significant X-ray emission at level consistent with the result of Cominsky et al. (1994).

The PSR B1259–63/SS 2883 system was observed with the *ASCA* satellite at six different orbital positions (hereafter *ASCA* obs 1 through *ASCA* obs 6) and with the OSSE instrument onboard the *CGRO* satellite at two different orbital positions: one near periastron and the second near apastron (hereafter OSSE obs A and OSSE obs B). *ASCA* observations 1–3 have been previously reported by Kaspi et al. (1995), *ASCA* obs 4 has been reported by Hirayama et al. (1996), and OSSE obs A has been discussed by Grove et al. (1995). In Figure 1 we provide a schematic drawing of the pulsar’s orbit around the systemic center of mass, together with the approximate location of the pulsar during all six *ASCA* observations, the three *ROSAT* observations reported by Cominsky et al. (1994) and Greiner et al. (1995), and the two OSSE observations. Also, for completeness, Table 1 gives a summary of the six *ASCA* and two OSSE observations and of the orbital geometry for an assumed Be star mass $M_c = 10 M_{\odot}$.

In this paper, we present the new *ASCA* data taken in *ASCA* obs 5 and *ASCA* obs 6, which were obtained near apastron, at phases similar to the *ROSAT* observations which occurred one 3.4 yr orbital cycle earlier (Cominsky et al. 1994; Greiner et al. 1995). We also present the OSSE obs B apastron results. The observations provide the X-ray luminosity in the 2 – 10 keV band at apastron which places constraints on the theoretical models (e.g. Tavani, Arons, & Kaspi 1994; Tavani & Arons 1997). Also, using the apastron observations we can attain maximum sensitivity

to pulsed magnetospheric X-ray emission from the pulsar, as X-ray emission from the binary interaction is at a minimum.

2. Observations

The *ASCA* satellite (Tanaka et al. 1994) carries four X-ray telescopes (Serlemitsos et al. 1995), with two X-ray CCD cameras (SIS hereafter) at two of their focal planes, and two gas scintillation imaging proportional counters (GIS hereafter, Ohashi et al. 1996) at the other two. The SIS detectors cover the energy range from 0.4 keV to 12 keV with an $11' \times 11'$ square field of view in 1-CCD mode, and the GIS detectors cover from 0.7 keV to 15 keV with a circular field of view of $25'$ radius. As with the four earlier *ASCA* observations, during *ASCA* obs 5 and *ASCA* obs 6, the two SIS detectors were operated in 1-CCD faint mode with a time resolution of 4 s. *ASCA*'s two GIS detectors were in PH mode with time resolution better than 4 ms, high enough to potentially study the 48 ms pulsations from PSR B1259–63.

The OSSE instrument consists of four large-area NaI(Tl)–CsI(Na) phoswich detector systems (Johnson et al. 1993) and covers the energy range from 50 keV to 10 MeV with good spectral resolution, and a field of view of approximately $3^\circ.8 \times 11^\circ.4$. OSSE had previously observed this object in 1994 January at periastron. In both observations, care was taken to minimize the effect of the galactic diffuse continuum emission and to avoid nearby bright point sources, such as the X-ray binaries GX 301–2, Cen X-3, and 2S 1417–624. The observations have similar orientations with respect to the galactic plane and similar background fields of view, and should therefore be subject to similar, minimal systematic effects. For the two week OSSE observation, spectra were accumulated in a sequence of two-minute measurements of the source field alternated with two-minute, offset-pointed measurements of background fields. In a total exposure time of 4.8×10^5 s, the highest-quality data were

collected on the source field, with an approximately equal time on the background fields. Simultaneously with the spectroscopy data, count-rate samples in eight energy bands at 8-ms resolution were collected to search for pulsed emission at the radio period.

One possible systematic effect is the inclusion of flux from the serendipitous source AX J1302–64, in the OSSE data. This weak source is seen in both the *ROSAT* data (Greiner et. al. 1995) and the *ASCA* data (Kaspi et al. 1995; Hirayama et al. 1996), but does not contaminate either analysis due to the imaging nature of the instruments. It is possible, however, that the source has flux in the OSSE bandpass, which could have added to that detected in this region in the periastron OSSE obs A data, although the required spectrum would be unusual for an accreting binary. We argue that the correlated variability seen in the *ASCA* and OSSE observations, in which the flux at periastron is more than a factor of ten greater than that detected near apastron in both instruments, makes it unlikely (but not impossible) that the OSSE obs A flux arises from AX J1302–64. A detailed analysis of AX J1302–64 will be presented elsewhere.

3. Data Analysis & Results

3.1. Spectral Results from *ASCA* data

In both observations *ASCA* obs 5 and *ASCA* obs 6, the PSR B1259–63/SS 2883 system was clearly detected with both SIS and GIS detectors. The observed positions of the X-ray source were coincident with the position of PSR B1259–63 to within $1'$, the accuracy of the attitude determination of the *ASCA* satellite. The method of analysis used to reduce the data from *ASCA* obs 5 and *ASCA* obs 6 is identical to that used for the first four *ASCA* observations (Kaspi et al. 1995; Hirayama et al. 1996).

After subtracting the background spectra, the source spectra from the combined *ASCA* GIS and SIS data taken in *ASCA* obs 5 and *ASCA*

obs 6 were fitted with a single power law model with photoelectric absorption, using XSPEC, a software package for X-ray spectral analyses. For completeness, the results of the independent three-parameter fits with the single power law model are given in Table 2 for all six *ASCA* observations. We also fitted the data with a thermal bremsstrahlung model with photoelectric absorption. In all cases, reduced χ^2 -values were only slightly higher for the thermal model compared with that for the power-law model, and we could not rule out the former on the basis of the *ASCA* observations alone. No evidence was found for any line features in the spectra. The upper limits for Iron K emission line at 6.4 keV, 6.7 keV, or 6.9 keV flux are listed in Table 2. The spectral fits with a thermal bremsstrahlung model result in plasma temperatures of 6 – 14 keV, at which Iron K emission lines are expected. Since none were detected, the absence of these lines argues in favor of the power law model.

Due to the weak detections at apastron, the X-ray photon indices and column densities in Table 2 are consistent with the entire range of values observed at periastron. In Figures 2 and 3 the changes in the photon index and the flux are plotted against the binary separation, assuming masses of $1.4 M_{\odot}$ for PSR B1259–63 and $10 M_{\odot}$ for SS 2883. The X-ray flux at apastron is ~ 10 times smaller than that near periastron. In this figure, we also show luminosity results from the previous X-ray missions (Makino & Aoki 1994; Cominsky et al. 1994; Greiner et al. 1995) converted into the 1–10 keV band, taking into account the best-fit photon indices and their errors.

3.2. Search for X-ray Pulsations in the *ASCA* data

We have searched the obs 5 and obs 6 data for evidence that the X-ray emission from the PSR B1259–63/SS 2883 system is pulsed at the 48 ms radio period using the same procedures followed by Kaspi et al. (1995) and Hirayama et al. (1996). These procedures were: 1) epoch

folding; 2) Z_n^2 test (Buccheri et al. 1983); 3) search in $P - \dot{P}$ space (Kaspi et al. 1995). The Z_n^2 test is used to detect the presence of up to n -th harmonic components of the pulsations (See Buccheri et al. 1983 for details). In the $P - \dot{P}$ search, pulsations are sought over a certain range of pulse period P and period derivative \dot{P} , around the P and \dot{P} estimated by radio timing observations (See §3.2.2 in Kaspi et al. 1995 for details).

The first two searches were done within $\pm 1\mu\text{s}$ from the expected pulse period of PSR B1259–63, as determined by Manchester et al. (1995) with the radio observations. Even though Wex et al. (1998) showed that the timing model for PSR B1259–63 by Manchester et al. (1995) does not fit the radio data obtained after MJD 49600, the period range we chose was wide enough to cover the entire range of possible periods. Searches for pulsations using the epoch-folding method were also done with a varying number of phase bins (8, 16, and 32) in order to ensure sensitivity to a variety of pulse profiles. The Z_n^2 tests were performed for the harmonic numbers $n = 1, 2, 3$, and 4. In addition, searches in the 0.5–2 keV and 2–10 keV bands were performed individually to detect possible narrow-band pulsations.

In conclusion, we detected no X-ray pulsations at the radio period, using any pulse searching technique. The upper limits to the pulsed component were estimated using the epoch-folding method described in Leahy et al. (1983) and are listed in Table 3. The limits were estimated by the pulsation searches with the epoch-folding method with $j = 32$ for three energy bands: 0.5–10 keV (full band), 0.5–2 keV, and 2–10 keV. The Z^2 searches (Buccheri et al. 1983) yielded similar results. In the table, upper limits on the amplitude of counting rates, AN_{γ} divided by net exposure time, are also listed.

3.3. OSSE Data Analysis and Results

The method of analysis was similar to that used for the periastron data, and is described more fully by Grove et al. (1995). No statistically significant unpulsed emission is detected by OSSE from PSR B1259–63 near apastron. Upper limits in several energy bins spanning 50 keV to 10 MeV are shown in Figure 4, together with the *ASCA* binned data for both obs 5 and obs 6. Also shown for comparison are the *ASCA* obs 1–4 and OSSE obs A periastron spectra, which have fluxes about ten times greater. At periastron, OSSE detected emission between 50 keV and \simeq 200 keV at \simeq 5 σ significance, as reported by Grove et al. (1995). Based on nearby measurements of the diffuse emission and on galactic symmetry, Grove et al. argued that the positive detection at periastron was probably not due to residual galactic emission. The null detection we report here strengthens this argument, and severely restricts the possibility that small-scale, local fluctuations in the diffuse emission could have been responsible for the observed flux at periastron.

4. Discussion

Our results from studying the soft and hard X-ray emission from the PSR B1259–63/SS 2883 system can be summarized as follows: 1) the X-ray emission is non-thermal and unpulsed for entire orbit (Kaspi et al. 1995; Hirayama et al. 1996; this paper), and especially at periastron, is characterized by a power-law spectrum which extends from 1 keV to up to 200 keV with a single photon index of \approx 2 (Grove et al. 1995); 2) the photon index varies slightly with orbital phase (Fig. 2); 3) the X-ray luminosity in the 1–10 keV band varies with orbital phase by about an order of magnitude, from \sim 10³⁴ erg s^{−1} at periastron to \sim 10³³ erg s^{−1} at apastron (assuming that the distance to the system is 2 kpc) (Fig. 3); 4) the observed X-ray luminosity at the apastron passage in 1995 (this paper) is consistent with that

at the previous apastron passage in 1992 (Cominsky et al. 1994; Greiner et al. 1995). In addition, a recent analysis of data obtained with the ASM instrument on the *RXTE* satellite near the 1997 periastron passage yielded an upper limit to the X-ray flux of $(0.5 \pm 2.4) \times 10^{-11}$ erg s^{−1} cm^{−2} in the 2–10 keV band (Kaspi & Remillard 1998), which is also consistent with the *ASCA* results at periastron by Kaspi et al. (1995).

The consistencies in X-ray luminosity at the two apastron passages (*ROSAT* obs 1, 2, and 3 versus *ASCA* obs 5 and 6) and at the two periastron passages (*ASCA* obs 2 versus *RXTE*/ASM) support the idea that the observed time variability in the X-ray luminosity is a binary modulation, i.e., variation due to the change in the pulsar’s position in the binary system. Therefore, a model in which the X-ray emission arises from only one of the binary components, such as emission from cooling neutron star surface, is unlikely to explain the observed data. Instead, a model that invokes interaction between the pulsar and the Be star is more likely to explain the observed orbital phase-dependent time variability in X-ray luminosity.

Binary modulation of the X-ray luminosity and the observed photon index can quantitatively be interpreted with the non-thermal diffuse nebular emission model of Tavani & Arons (1997). In this model, the observed X-rays are due to synchrotron emission from e^\pm pairs with $\gamma = 10^6$ – 10^7 accelerated at a shock front formed between the pulsar wind from PSR B1259–63 and the stellar wind from SS 2883 (Tavani et al. 1994; Kaspi et al. 1995; Hirayama et al. 1996; Tavani & Arons 1997). Alternative explanations of the X-ray emission from the binary system have also been proposed, such as emission from accretion onto neutron star surface and emission from material captured outside the pulsar’s light-cylinder (King & Cominsky et al. 1994). These mechanisms predict thermal bremsstrahlung emission from gaseous material heated through the accretion process, which is less likely to be consistent

with our data.

Results from the *ASCA* and OSSE observations near periastron in 1994 (Kaspi et al. 1995; Grove et al. 1995) indicate that a shock-powered emission model provides a natural way to account for all the observations (Tavani et al. 1994; Tavani & Arons 1997). Tavani & Arons (1997) showed that shock-powered emission with radiative cooling explains the X-ray properties observed around periastron, such as the power-law spectrum extending to 200 keV, the spectral softening at periastron, and the luminosity variation near periastron. In addition, the results of *ASCA* obs 4 through obs 6 (Hirayama et al. 1996; this paper) show qualitative agreement with the predictions of this model for the X-ray luminosity and photon index. On the other hand, accretion-powered emission models cannot explain the moderate X-ray luminosity of $\sim 10^{34}$ erg s $^{-1}$ at periastron, because the strong magnetic field of the pulsar will inhibit accretion until the mass flux is sufficiently strong to overcome the centrifugal barrier (Stella, White and Rosner 1986). Once accretion occurs, a significantly larger X-ray luminosity should be observed ($\sim 10^{37}$ erg s $^{-1}$). Also, as Grove et al. (1995) discussed, a single power-law spectrum from 1 keV to 200 keV cannot be explained by thermal emission from heated accreting matter.

Based on the shock emission model by Tavani & Arons (1997), the power-law spectrum with photon index $\alpha \approx 1.6$, observed when the pulsar was farther than 1000 lt-s from the Be star, required the shock acceleration mechanism to create e^\pm pairs with an energy spectrum $N(\gamma) \propto \gamma^{-2}$ just behind the shock front (Hirayama et al. 1996). In this context, the apparent softening of the spectral index can be understood in terms of enhanced radiative cooling (Kaspi et al. 1995; Hirayama et al. 1996; Tavani & Arons 1997). The decrease in X-ray flux near periastron provides additional evidence in favor of this explanation.

The *ASCA* obs 5 data set the tightest upper

limit yet on pulsed X-ray magnetospheric X-ray emission from PSR B1259–63. From Table 3, the pulsed luminosity is $< 3 \times 10^{31}$ erg s $^{-1}$ at the 99% confidence level, assuming a distance of 2 kpc and 1 sr beaming angle. Saito (1997) and Saito et al. (1998) systematically studied the pulsed luminosity from spin-powered pulsars in the X-ray band based on the *ASCA* observations and found an empirical relationship between pulsed luminosity and spin-down luminosity given by $L_{X(\text{pulsed})} = 10^{34} \times (\dot{E}_{\text{rot,38}})^{3/2}$ erg s $^{-1}$, where $L_{X(\text{pulsed})}$ is the pulsed luminosity in the 2 – 10 keV band for 1 sr beaming, and $\dot{E}_{\text{rot,38}}$ is the spin-down luminosity in units of 10^{38} erg s $^{-1}$. Based on this relationship, the pulsed luminosity from PSR B1259–63 is predicted to be $\sim 7.5 \times 10^{30}$ erg s $^{-1}$, which is smaller than our best upper limit. Thus, the result is not yet strongly constraining.

This research was partially supported by NASA through the grant NAG 5-2730. MH acknowledges support from Research Fellowships of the Japan Society for the Promotion of Science for Young Scientists. LRC acknowledges support by NASA through the grants NAG 5-2948 and NAG 5-2032 for analysis of *ASCA* and OSSE data. JEG acknowledges support by NASA contract S-10987-C for OSSE data analysis.

REFERENCES

Buccheri, R., et al. 1983, *A&A*, 128, 245

Cominsky, L., Roberts, M., & Johnston, S. 1994, *ApJ*, 427, 978

Greiner, J., Tavani, M., & Belloni, T. 1995, *ApJ*, 441, L43

Grove, J. E., Tavani, M., Purcell, W. R., Johnston, W. N., Kurfess, J. D., Strickman, M. S., & Arons, J. 1995, *ApJ*, 447, L113

Hirayama, M., Nagase, F., Tavani, M., Kaspi, V. M., Kawai, N., & Arons, J. 1996, *PASJ*, 48, 833

Johnson, W. N., et al. 1993, *ApJS*, 86, 693

Johnston, S., Lyne, A. G., Manchester, R. N., Kniffen, D. A., D'Amico, N., Lim, J., & Ashworth, M. 1992a, *MNRAS*, 255, 401

Johnston, S., Manchester, R. N., Lyne, A. G., Bailes, M., Kaspi, V. M., Guojun, Q., & D'Amico, N. 1992b, *ApJ*, 387, L37

Johnston, S., Manchester, R. N., Lyne, A. G., Nicastro, L., & Spyromilo, J. 1994, *MNRAS*, 268, 430

Kaspi, V. M., Tavani, M., Nagase, F., Hirayama, M., Hoshino, M., Aoki, T., Kawai, N., & Arons, J. 1995, *ApJ*, 453, 424

Kaspi, V. M., & Remillard, R. A. 1998, *Proceedings of the Symposium “Neutron Stars and Pulsars” held in Tokyo Japan, November 17-20, 1997*, Universal Academy Press, in press

King, A., & Cominsky, L. 1994, *ApJ*, 435, 411.

Leahy, D. A., Darbro, W., Elsner, R. F., Weiskopf, M. C., Sutherland, P. G., Kahn, S., & Grindlay, J. E. 1983, *ApJ*, 266, 160

Makino, F., & Aoki, T. 1994, private communication

Manchester, R. N., Johnston, S., Lyne, A. G., D'Amico, N., Bailes, M., & Nicastro, L. 1995, *ApJ*, 445, L137

Ohashi, T., et al. 1996, *PASJ*, 48, 157

Saito, Y. 1997, Doctoral thesis, University of Tokyo, March 1997

Saito, Y., Kawai, N., Kamae, T., & Shibata, S. 1998, *Proceedings of the Symposium “Neutron Stars and Pulsars” held in Tokyo Japan, November 17-20, 1997*, Universal Academy Press, in press

Serlemitos, P. J., et al. 1995, *PASJ*, 47, 105

Stella, L., White, N. E., & Rosner, R. 1986, *ApJ*, 308, 669

Tanaka, Y., Inoue, H., & Holt, S. S. 1994, *PASJ*, 46, L37

Tavani, M. & Arons, J. 1997, *ApJ*, 477, 439

Tavani, M., Arons, J., & Kaspi, V. M. 1994, *ApJ*, 433, L37

Taylor, J. H., & Cordes, J. M. 1993, *ApJ*, 411, 674

Wex, N., Johnston, S., Manchester, R. N., Lyne, A. G., Stappers, B. W., & Bailes, M. 1998, *MNRAS*, in press

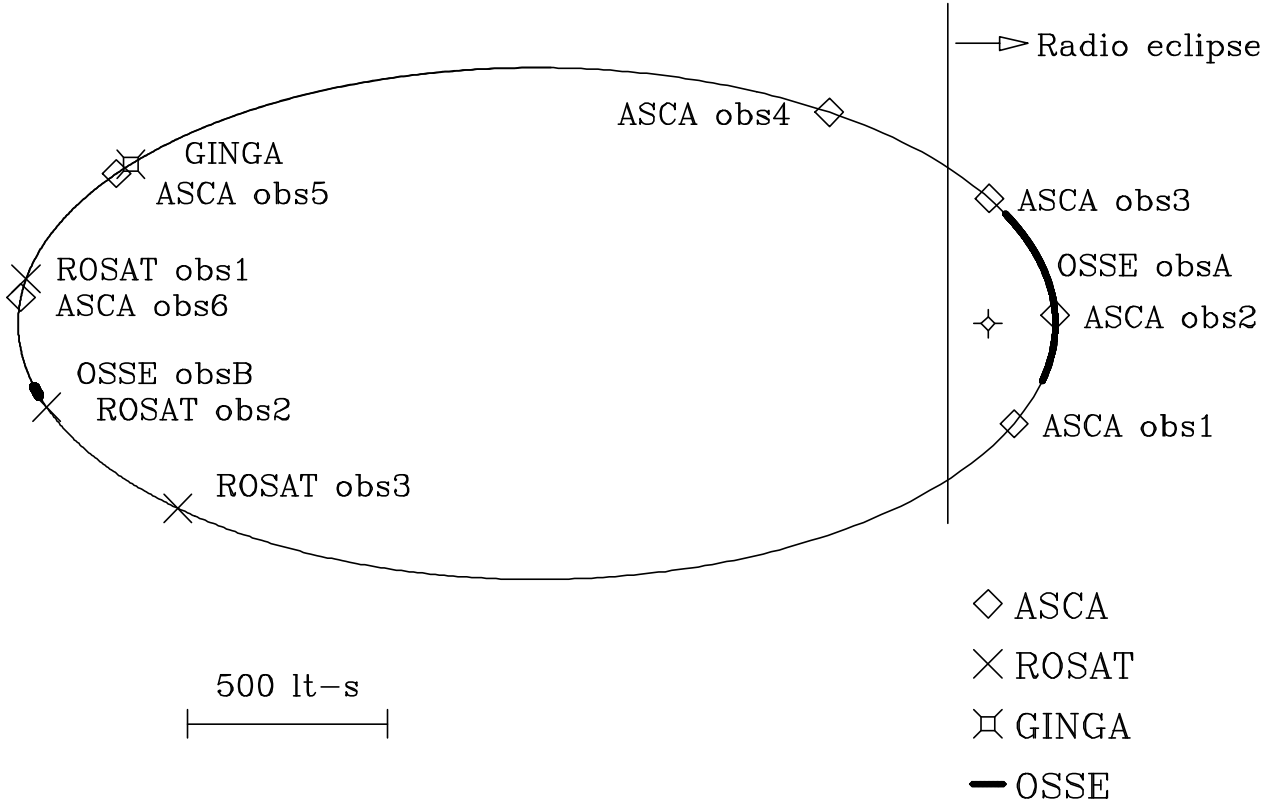


Fig. 1.— Binary orbit of the PSR B1259–63/SS 2883 system. An elliptical line shows the orbit of PSR B1259–63 and a diamond with a cross in the ellipse indicates the center of gravity of the system. The figure also shows the positions of PSR B1259–63 when observed with *ASCA* (this work), *ROSAT* (Cominsky et al. 1994; Greiner et al. 1995), and *Ginga* (Makino & Aoki 1994) at various locations on the orbit. The OSSE instrument on the *CGRO* satellite observed PSR B1259–63 for three weeks during the periastron passage in 1994 and for two weeks near apastron in 1995/6 as indicated with thick lines on the orbit. When the pulsar is at the right side of the vertical line in the figure, no radio pulsations are detected (Johnston et al. 1992b).

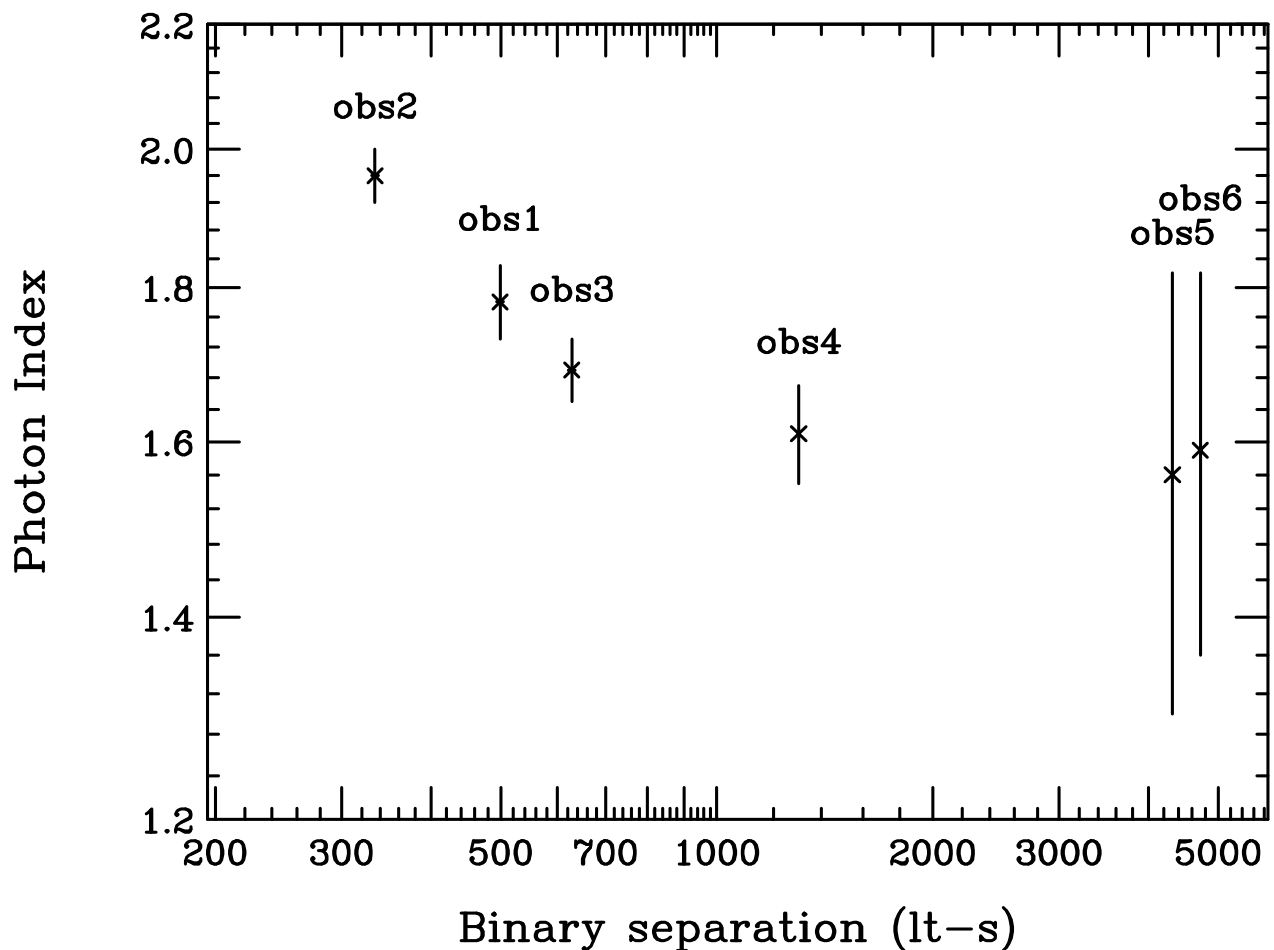


Fig. 2.— Photon indices of the PSR B1259–63/SS 2883 system from *ASCA* obs 1 through *ASCA* obs 6 are plotted against binary separation assuming $1.4 M_{\odot}$ for PSR B1259–63 and $10 M_{\odot}$ for SS 2883.

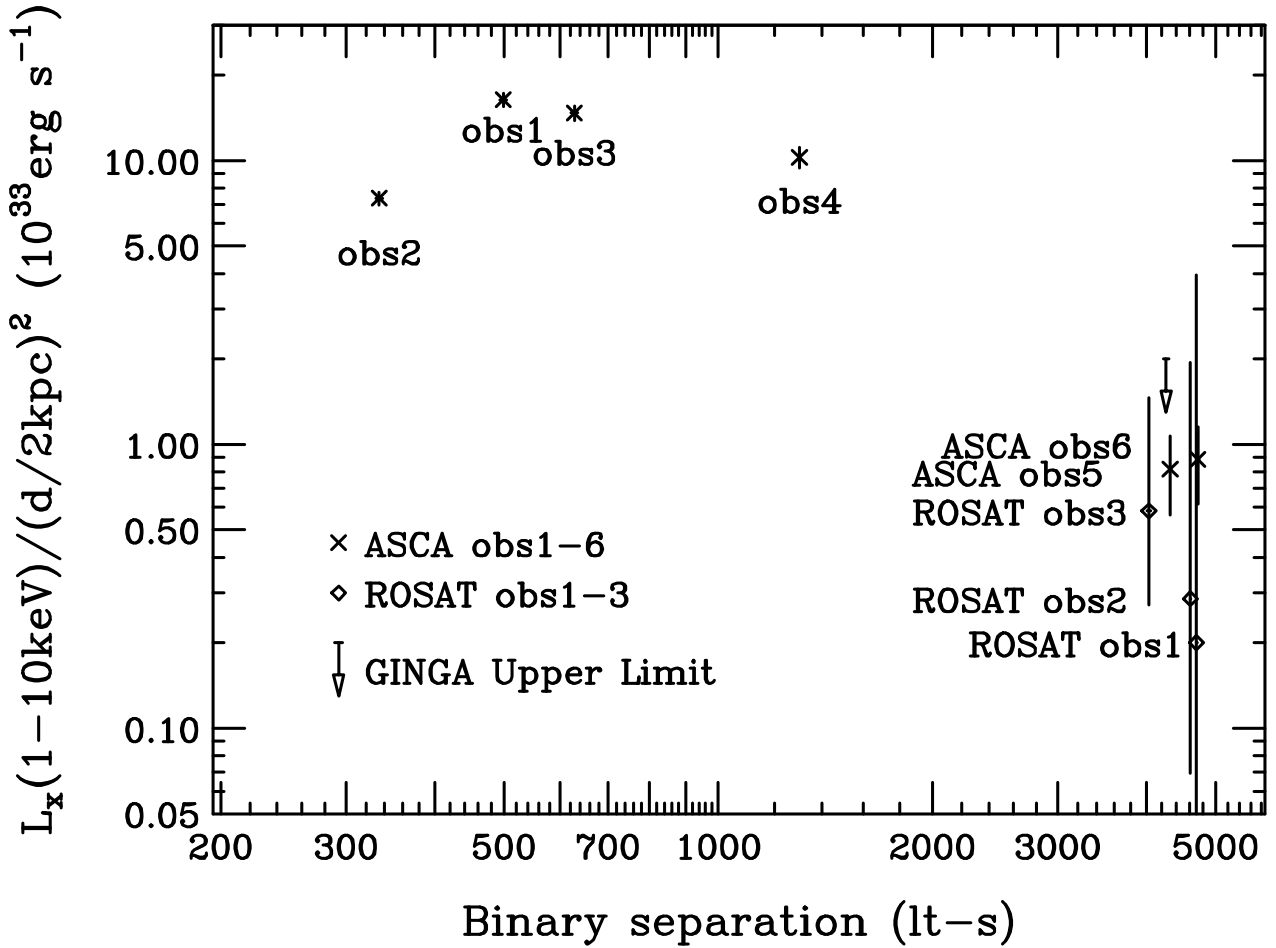


Fig. 3.— Luminosities of the PSR B1259–63/SS 2883 system from *ASCA* obs 1 through *ASCA* obs 6 are plotted against a binary separation assuming masses of $1.4 M_{\odot}$ for PSR B1259–63 and $10 M_{\odot}$ for SS 2883, and a distance to the PSR B1259–63/SS 2883 system $d = 2$ kpc. In the figure results from the previous X-ray missions are also plotted (Makino & Aoki 1994; Cominsky et al. 1994; Greiner et al. 1995) with the luminosities in the literature extrapolated to the 1–10 keV band.

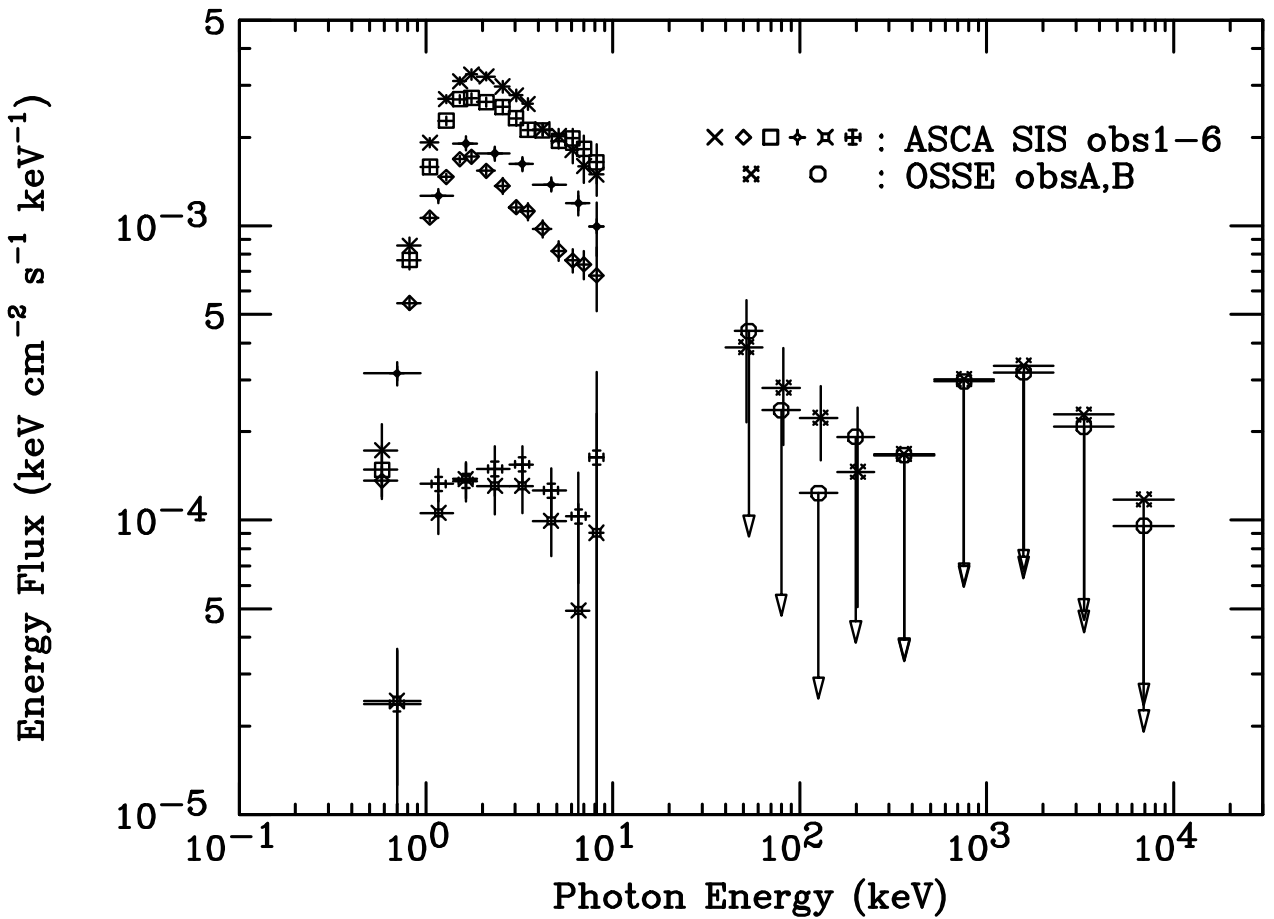


Fig. 4.— Unfolded spectra obtained for the six *ASCA* observations (Kaspi et al. 1996; Hirayama et al. 1996; this paper) and the two OSSE observations (Grove et al. 1995; this paper). For the figure, masses of $1.4 M_{\odot}$ for PSR B1259–63 and $10 M_{\odot}$ for SS 2883, and a distance to the PSR B1259–63/SS 2883 system $d = 2$ kpc are assumed. Note that the exposure times for the OSSE observations differ (see table 1).

TABLE 1

GEOMETRY OF THE PSR B1259–63/SS 2883 SYSTEM NEAR THE *ASCA* AND OSSE OBSERVATIONS

Observation	MJD	True Anomaly ^a	$s(10^{12} \text{ cm})^b$	s/R_c^c	Reference
<i>ASCA</i> obs 1	49349	−75°	15	36	Kaspi et al. 1995
	49362	8°	10	24	Kaspi et al. 1995
	49378	90°	18	45	Kaspi et al. 1995
	49411	127°	39	93	Hirayama et al. 1996
	49755	170°	130	310	this paper
	49942	178°	140	340	this paper
OSSE obs A	49355 – 49375	$-47^\circ \sim +81^\circ$	10 – 16	24 – 39	Grove et al. 1995
	50071 – 50084	−176°	140	340	this paper

^aTrue anomaly is zero at periastron.^bBinary separation for assumed Be star and pulsar masses of $M_c=10 M_\odot$ and $M_p=1.4 M_\odot$.^cAssuming a companion radius R_c of $6R_\odot$.

TABLE 2

MODEL PARAMETERS FOR THE *ASCA* OBSERVATIONS OF THE PSR B1259–63/SS 2883 SYSTEM

<i>ASCA</i> Dataset	N_{H}^a (10^{22} cm^{-2})	Photon Index ^a	1–10 keV Flux ^a ($10^{-11} \text{ erg cm}^{-2} \text{ s}^{-1}$)	χ^2_ν	Fe Emission-Line Flux ^b ($10^{-5} \text{ photons cm}^{-2} \text{ s}^{-1}$)
obs 1	0.60(4)	1.78(5)	3.43(19)/2.96(16)	0.97	< 1.7
obs 2	0.58(3)	1.96(4)	1.54(8)/1.42(7)	0.96	< 1.5
obs 3	0.58(4)	1.69(4)	3.08(18)/2.76(16)	1.22	< 4.0
obs 4	0.56(6)	1.61(6)	2.15(18)/1.88(16)	0.98	< 2.9
obs 5	0.5(3)	1.6(3)	0.17(5)/0.18(5)	0.71	< 0.7
obs 6	0.5(2)	1.6(2)	0.19(6)/0.18(5)	0.84	< 1.3

^aNumbers in parentheses represent 90% confidence interval uncertainties in the last digit quoted. The uncertainties quoted are statistical, and do not include any contribution for unknown systematic calibration errors.^bUpper limits with 99 % confidence assuming a narrow emission line (of equivalent width of 1 eV) at 6.4 keV, 6.7 keV, or 6.9 keV.

TABLE 3

UPPER LIMITS ON X-RAY PULSATIONS OBTAINED FROM THE *ASCA* OBSERVATIONS^a

<i>ASCA</i> Dataset	0.5–10 keV	0.5–2 keV	2–10 keV
obs 1	8.71% (0.0338)	15.1% (0.0204)	11.8% (0.0280)
obs 2	7.58% (0.0155)	13.4% (0.0114)	10.7% (0.0125)
obs 3	8.38% (0.0302)	18.4% (0.0243)	11.3% (0.0253)
obs 4	15.1% (0.0378)	22.2% (0.0187)	15.3% (0.0249)
obs 5	29.1% (0.0110)	44.8% (0.00642)	36.3% (0.00828)
obs 6	29.9% (0.0125)	49.6% (0.00783)	37.0% (0.00902)

^aUpper limits in the table are estimated with 99% confidence, being given as the fractional amplitude of an assumed sinusoidal pulse. Counting rates corresponding to the upper limits are also listed in parentheses in the table in units of photons s⁻¹. Note that, due to the smaller luminosities in *ASCA* obs 5 and *ASCA* obs 6, these data give higher fractional upper limits, but stricter upper limits for the pulsed flux.